

# Superfluidity of metastable glassy bulk *para*-hydrogen at low temperature

O. N. Osychenko,<sup>1</sup> R. Rota,<sup>2</sup> and J. Boronat<sup>1</sup><sup>1</sup>*Departament de Física i Enginyeria Nuclear, Universitat Politècnica de Catalunya, Campus Nord B4-B5, E-08034, Barcelona, Spain*<sup>2</sup>*Dipartimento di Fisica, Università di Trento and INO-CNR BEC Center, I-38123 Povo, Trento, Italy*

(Received 30 March 2012; revised manuscript received 21 May 2012; published 13 June 2012)

Molecular *para*-hydrogen ( $p$ -H<sub>2</sub>) has been proposed theoretically as a possible candidate for superfluidity, but the eventual superfluid transition is hindered by its crystallization. In this work, we study a metastable noncrystalline phase of bulk  $p$ -H<sub>2</sub> by means of the path integral Monte Carlo method in order to investigate at which temperature this system can support superfluidity. By choosing accurately the initial configuration and using a noncommensurate simulation box, we have been able to frustrate the formation of the crystal in the simulated system and to calculate the temperature dependence of the one-body density matrix and of the superfluid fraction. We observe a transition to a superfluid phase at temperatures around 1 K. The limit of zero temperature is also studied using the diffusion Monte Carlo method. Results for the energy, condensate fraction, and structure of the metastable liquid phase at  $T = 0$  are reported and compared with the ones obtained for the stable solid phase.

DOI: [10.1103/PhysRevB.85.224513](https://doi.org/10.1103/PhysRevB.85.224513)

PACS number(s): 67.63.Cd, 67.80.ff, 67.10.Ba, 02.70.Ss

## I. INTRODUCTION

Superfluidity and Bose-Einstein condensation (BEC) have been stunningly shown in metastable dilute alkali gases, magnetically confined at ultralow temperatures.<sup>1</sup> The extreme diluteness of these gases allows for the achievement of BEC with an almost full occupation of the zero-momentum state that has been possible to observe and measure quite easily. This contrasts with the difficulties encountered in the measure of the condensate fraction in liquid <sup>4</sup>He, which amounts to only 8% at the equilibrium density.<sup>2</sup> However, liquid <sup>4</sup>He is a stable superfluid below the lambda transition  $T_\lambda = 2.17$  K and is therefore a more easily accessible system. Before the blowup produced in the field of quantum fluids by the first experimental realization of BEC gases, liquid helium was the only paradigm of a superfluid. For a long time, there has been great interest in the search for superfluid condensed phases other than liquid helium. Spin-polarized atomic deuterium and tritium are predicted to be fermionic and bosonic liquids, respectively, in the limit of zero temperature.<sup>3,4</sup> However, their experimental study has proven to be very elusive due to their high recombination rate, and only the case of atomic hydrogen, whose ground state is a gas, has been experimentally driven to its BEC state.<sup>5</sup> The next candidate for superfluidity is molecular hydrogen, which has been studied for a long time.<sup>6</sup> This seems *a priori* an optimal system due to its very light mass but it crystallizes at relatively high temperature as a consequence of the intensity of its intermolecular attraction, without exhibiting any superfluid transition in the liquid phase. In the present work, we study the properties of metastable liquid or glass molecular hydrogen at very low temperatures using quantum Monte Carlo methods.

In 1972, Ginzburg and Sobyenin<sup>7</sup> proposed that any Bose liquid should be superfluid below a certain temperature  $T_\lambda$ , unless it solidifies at temperature  $T_f$  higher than  $T_\lambda$ . To give a first estimation of  $T_\lambda$ , they used the ideal Bose gas theory, obtaining

$$T_\lambda = 3.31 \frac{\hbar^2}{g^{2/3} m k_B} \rho^{2/3}, \quad (1)$$

where  $m$  is the atomic mass,  $g$  is the spin degeneracy,  $k_B$  is the Boltzmann constant, and  $\rho$  is the density of the system. Ginzburg and Sobyenin proposed molecular *para*-hydrogen ( $p$ -H<sub>2</sub>) as a plausible candidate for superfluidity: Being a spinless boson ( $g = 1$ ) with a small mass,  $p$ -H<sub>2</sub> should undergo a superfluid transition at a relatively high temperature [according to Eq. (1),  $T_\lambda \simeq 6$  K].

The estimation of  $T_\lambda$ , given by Eq. (1), is clearly inaccurate in the case of dense liquids because it cannot account for the observed dependence of  $T_\lambda$  with the density. In fact,  $T_\lambda$  slightly decreases in liquid <sup>4</sup>He when  $\rho$  increases, a manifestly opposite behavior to the increase with  $\rho^{2/3}$  given by the ideal gas formula (1). In order to provide a more reasonable estimation of  $T_\lambda$ , Apenko<sup>8</sup> proposed a phenomenological prescription for the superfluid transition, similar to the Lindemann criterion for classical crystal melting. In this way, he was able to take into account quantum decoherence effects due to the strong interatomic potential and to relate the critical temperature for superfluidity with the mean kinetic energy per particle above the transition. For  $p$ -H<sub>2</sub>, he concluded that  $T_\lambda$  should vary between 1.1 and 2.1 K, depending on the density of the system.

Superfluid  $p$ -H<sub>2</sub> is not observed in a stable form because it crystallizes at temperature  $T_f = 13.8$  K, which is significantly higher than the expected  $T_\lambda$ . Several studies about crystal nucleation in  $p$ -H<sub>2</sub> have been performed in order to understand if the liquid can enter a supercooled phase (i.e., a metastable phase in which the liquid is cooled below its freezing temperature without forming a crystal). Maris *et al.*<sup>9</sup> calculated the rate  $\Gamma(T)$  of homogeneous nucleation of the solid phase from the liquid as a function of the temperature  $T$ , showing a maximum of  $\Gamma$  around  $T = 7$  K and a rapid decrease at lower temperature. This suggests that, if it would be possible to supercool the liquid through the range where  $\Gamma$  is large, one might be able to reach a low-temperature region where the liquid is essentially stable. However, recent experiments have indicated that, even at  $T \sim 9$  K, the rate of crystal growth is so high that the liquid phase freezes quickly into a metastable polymorph crystal.<sup>10</sup>

Even though several supercooling techniques have been proposed to create a metastable liquid phase in bulk  $p$ -H<sub>2</sub>,<sup>11–13</sup>

none of them has proven so far to be successful and no direct evidence of superfluidity has been detected. However, there are evidences of superfluidity in several spectroscopic studies of small doped  $p$ -H<sub>2</sub> clusters. In 2000, Grebenev *et al.*<sup>14</sup> analyzed the rotational spectra of a linear carbonyl sulfide (OCS) molecule surrounded by 14–16  $p$ -H<sub>2</sub> molecules absorbed in a larger helium droplet, which fixes the temperature of the cluster. When  $p$ -H<sub>2</sub> is immersed in a <sup>4</sup>He droplet ( $T = 0.38$  K), the measured spectra show a peak indicating the excitation of angular momentum around the OCS axis. On the other hand, if the small  $p$ -H<sub>2</sub> cluster is put inside a colder <sup>4</sup>He-<sup>3</sup>He droplet ( $T = 0.15$  K), the peak disappears: The OCS molecule is then able to rotate freely inside the hydrogen cluster, pointing to the superfluidity of the surrounding  $p$ -H<sub>2</sub> molecules. These results have been confirmed in a later experiment on small  $p$ -H<sub>2</sub> clusters doped with carbon dioxide.<sup>15</sup> From a precise analysis of the rotational spectra, it has been possible to measure the effective momentum of inertia of these small systems, and thus of their superfluid fraction  $\rho_s$ , providing a clear evidence of superfluidity in clusters made up of  $N \leq 18$   $p$ -H<sub>2</sub> molecules. These clusters are too small to extract reliable predictions of a metastable liquid phase and larger clusters would be desirable. To this end, Kuyanov-Prozument and Vilesov<sup>16</sup> have been able to stabilize liquid clusters with an average size of  $N \approx 10^4$   $p$ -H<sub>2</sub> molecules down to temperature  $T = 2$  K, but they do not see any evidence of superfluidity. Other attempts of producing liquid  $p$ -H<sub>2</sub> well below  $T_f$  ( $T = 1.3$  K) are based on the generation of continuous hydrogen filaments of macroscopic dimensions.<sup>13</sup>

The search for a superfluid  $p$ -H<sub>2</sub> phase has been intense also from the theoretical point of view. The rather simple radial form of the  $p$ -H<sub>2</sub>- $p$ -H<sub>2</sub> interaction and the microscopic accuracy achieved by quantum Monte Carlo methods have stimulated a long-standing effort for devising possible scenarios where supercooled  $p$ -H<sub>2</sub> could be studied. In practically all the cases, the search is focused on systems of reduced dimensionality or in finite systems. Path integral Monte Carlo (PIMC) simulations of  $p$ -H<sub>2</sub> films adsorbed on a surface with impurities observed superfluidity for some arrangements of these impurities,<sup>17</sup> but these results were posteriorly questioned by other PIMC studies.<sup>18</sup> In a one-dimensional channel, like the one provided experimentally by narrow carbon nanotubes, it has been predicted a stable liquid phase in the limit of zero temperature.<sup>19</sup> The largest number of theoretical works have been devoted to the study of small clusters, both pure<sup>20–29</sup> and doped with impurities.<sup>30–32</sup> All these simulations show that  $p$ -H<sub>2</sub> becomes superfluid below a certain temperature  $T = 1$ – $2$  K and that the superfluid fraction depends on the number of molecules of the cluster. When the cluster becomes larger than a certain molecular number ( $N > 18$ – $25$ ), solidlike structures are observed and the superfluidity vanishes.

In the present work, we deliver a PIMC study of a metastable glass/liquid phase at very low temperature. Our main purpose has been to determine for the first time at which temperature this metastable phase becomes superfluid and the value of the superfluid density and condensate fraction close to this temperature. The simulations are carried out following schedules which are similar to the ones used in a recent study of a glass <sup>4</sup>He phase evolving from a normal to a superfluid

state (superglass).<sup>33</sup> Our results show that this transition temperature is  $T \simeq 1$  K, a value that is close to the Apenko estimation<sup>8</sup> and also close to the values observed in simulations of small clusters. As a complementary aspect, we address the calculation of the equation of state of the metastable liquid  $p$ -H<sub>2</sub> phase in the limit of zero temperature using the diffusion Monte Carlo (DMC) method. The simulation of the liquid phase in this limit is easier than at finite temperature and therefore DMC is able to provide accurate information on its main energetic and structure properties.

The rest of the paper is organized as follows. In Sec. II, we introduce the quantum Monte Carlo methods used in the study, the DMC and PIMC methods, and report specific details on how the simulations are carried out. Section III contains the results of the equation of state, structure properties, and condensate fraction of metastable liquid  $p$ -H<sub>2</sub> at zero temperature. PIMC results at finite temperature are reported in Sec. IV, and finally the main conclusions of the present work are discussed in Sec. V.

## II. QUANTUM MONTE CARLO METHODS

The H<sub>2</sub> molecule, which is composed of two hydrogen atoms linked by a covalent bond, is spherically symmetric in the *para*-hydrogen state (total angular momentum zero). The energy scale involved in electronic excitations ( $\sim 10^5$  K) is orders of magnitude larger than the intermolecular one ( $\sim 10^1$  K), thus modeling the  $p$ -H<sub>2</sub>- $p$ -H<sub>2</sub> interaction by means of a radial pair potential and considering the molecules as pointlike turns out to be justified upon the condition of low or moderate pressures. In this work, we have chosen the well-known and commonly used semiempirical Silvera-Goldman pair potential.<sup>34</sup> This potential has proved to be accurate at low temperature and in the pressure regimes in which we are interested.

The study in the limit of zero temperature has been performed with the DMC method. DMC is a first-principles method which can access exactly the ground state of bosonic systems. It is a form of Green's function Monte Carlo which samples the projection of the ground state from the initial configuration with the operator  $\exp[-(\mathcal{H} - E_0)\tau]$ . Here,  $\mathcal{H}$  is the Hamiltonian,

$$\mathcal{H} = -\frac{\hbar^2}{2m} \sum_{i=1}^N \nabla_i^2 + \sum_{1=i < j}^N V(r_{ij}), \quad (2)$$

$E_0$  is a norm-preserving adjustable constant, and  $\tau$  is the imaginary time. The simulation is performed by advancing in  $\tau$  via a combination of diffusion, drift, and branching steps on walkers  $\mathbf{R}$  (sets of  $3N$  coordinates) representing the wave function of the system.<sup>35</sup> The imaginary-time evolution of the walkers is “guided” during the drift stage by a guiding wave function  $\phi_G$ , which is usually a good guess for the wave function of the system. This function contains basic ingredients of the system as its symmetry, phase, and expected behaviors at short and long distances according to its Hamiltonian. Technically,  $\phi_G$  allows importance sampling and thus reduces the variance of the ground-state estimations. It is straightforward to show that for the Hamiltonian  $\mathcal{H}$  and any operator commuting with it, the expectation value is computed exactly within statistical error. Other diagonal operators which do not fulfill this condition

require a special treatment, known as pure estimation,<sup>36</sup> which also leads for this case to unbiased results.

The phase of the system is imposed within the typical imaginary-time length by the guiding wave function. This property of the DMC method is here a key point if we are pursuing an investigation of the properties of the metastable liquid  $p$ -H<sub>2</sub> phase. Then, for the liquid phase  $\phi_G$  is taken in a Jastrow form,

$$\phi_G(\mathbf{R}) = \prod_{1=i<j}^N f(r_{ij}), \quad (3)$$

with a two-body correlation function,<sup>37</sup>

$$f(r) = \exp \left[ -\frac{1}{2} \left( \frac{b}{r} \right)^5 - \frac{L}{2} \exp \left[ -\left( \frac{r-\lambda}{\Lambda} \right)^2 \right] \right]. \quad (4)$$

In order to compare the results obtained for the liquid phase with the ones corresponding to the stable hcp solid we have carried out some simulations with a guiding wave function of the Nosanow-Jastrow type,

$$\phi_G^s(\mathbf{R}) = \prod_{1=i<j}^N f(r_{ij}) \prod_{i=1}^N g(r_{iI}), \quad (5)$$

the set  $\{\mathbf{r}_I\}$  being the lattice points of a perfect hcp lattice. Optimal values for the parameters entering Eq. (4) are  $b = 3.68 \text{ \AA}$ ,  $L = 0.2$ ,  $\lambda = 5.24 \text{ \AA}$ , and  $\Lambda = 0.89 \text{ \AA}$  for the liquid phase, and  $b = 3.45 \text{ \AA}$ ,  $L = 0.2$ ,  $\lambda = 5.49 \text{ \AA}$ , and  $\Lambda = 2.81 \text{ \AA}$  for the solid one. The Nosanow term is chosen in Gaussian form,  $g(r) = \exp(-\gamma r^2)$ . The density dependence of the parameters in the Jastrow term is small, and neglected in practice when used in DMC, whereas the Nosanow term parameter  $\gamma$  is optimized for the whole range of densities. We have used 256 and 180 particles per simulation box for the liquid and hcp solid phases, respectively. The number of walkers and the time step have been adjusted to reduce any bias coming from them to the level of the statistical noise.

At finite temperature  $T$ , the microscopic description of the quantum system is made in terms of the thermal density matrix,  $\rho_N(\mathbf{R}', \mathbf{R}; \beta) = \langle \mathbf{R}' | e^{-\beta \mathcal{H}} | \mathbf{R} \rangle$ , with  $\beta = (k_B T)^{-1}$ . The partition function  $Z$ , which allows for a full description of the properties of a given system, satisfies the relation,

$$Z = \text{Tr}(e^{-\beta \mathcal{H}}) \simeq \int \prod_{i=1}^M d\mathbf{R}_i \rho_N(\mathbf{R}_i, \mathbf{R}_{i+1}; \varepsilon), \quad (6)$$

that relies on the convolution property of the density matrix. In Eq. (6),  $\varepsilon = \beta/M$  and the boundary condition  $\mathbf{R}_{M+1} = \mathbf{R}_1$  applies. The remarkable feature of Eq. (6), on which PIMC is based, is that one has access to information at a temperature  $T$  by convoluting density matrices at higher temperature  $MT$ .<sup>38</sup>

PIMC describes the quantum  $N$ -body system considering  $M$  different configurations  $\mathbf{R}_j$  of the same system, whose sequence constitutes a path in imaginary time. This means that the  $N$ -body quantum system is mapped onto a classical system of  $N$  ring polymers, each one composed by  $M$  beads. The different beads can be thought as a way to describe the delocalization of the quantum particle due to its zero-point motion. For sufficiently large  $M$ , one recovers the high-temperature density matrix, where it is legitimate to separate

the kinetic contribution from the potential one (primitive action). In this way, it is possible by applying Eq. (6) to reduce the systematic error due to the analytical approximation for  $\rho_N$  below the statistical uncertainty. However, the primitive action is too simple to study extreme quantum matter and a better choice for the action is fundamental to reduce both the complexity of the calculation and ergodicity issues. To this end, we have used a high-order Chin action<sup>39,40</sup> to obtain an accurate estimation of the relevant physical quantities with reasonable numeric effort even in the low-temperature regime, where the simulation becomes harder due to the large zero-point motion of particles. We have analyzed the dependence of the  $p$ -H<sub>2</sub> energy on the parameter  $\varepsilon$  and determined an optimal value  $\varepsilon = 1/60 \text{ K}^{-1}$  for which the bias coming from the use of a finite  $\varepsilon$  value is smaller than the characteristic statistical noise.

A relevant issue one has to deal with when approaching the low-temperature limit with PIMC simulations arises from the indistinguishable nature of the particles. In the path integral formalism, the exchanges between  $L$  different particles are represented by long ring polymers composed by  $L \times M$  beads. If we study a bosonic system like  $p$ -H<sub>2</sub>, the indistinguishability of the particles does not affect the positivity of the integrand function in Eq. (6) and the symmetry of  $Z$  can be recovered by the sampling of permutations between the ring polymers. In the present study, we have used the worm algorithm<sup>41</sup> which provides a very efficient sampling in permutation space.

The key aspect of the worm algorithm is to work in an extended configuration space, containing not only the usual diagonal configurations made up of ring polymers, but also off-diagonal configurations which are characterized by the presence of an open polymer (defined as the *worm*). By working with off-diagonal configurations, it is possible to sample the bosonic permutations by means of single-particle movements, like the *swap* update, whose acceptance rate can be made comparable to that of the other updates in the sampling of polymers. In order to fulfill this condition, it is important to optimize two parameters of the worm algorithm. The first of them is  $C$ , which regulates the acceptance probability of the movements switching from diagonal to off-diagonal configuration and vice versa. In our simulations, we choose  $C$  to get the number of sampled off-diagonal configurations to about 65%–70% of the total number of configurations. In this way, the system is allowed to spend enough time both in off-diagonal configurations, where the sampling of permutations is done, and in diagonal configurations, where relevant observables such as the energy or the superfluid density are evaluated. The second one is  $M_s$ , which is the number of beads rebuilt in the swap update. The parameter  $M_s$  has to be chosen as a compromise between a small value, which would make difficult the search of the partner of the worm in the swap movement, and a large value which would make difficult the reconstruction of the polymer once the partner has been chosen. In our simulations, we use  $M_s$  which maximizes the acceptance rate of the swap update: The typical value of  $M_s$  is about 10% of the number of beads  $M$ .

### III. ZERO-TEMPERATURE RESULTS

We have calculated the main properties of the metastable liquid and stable hcp solid phases of  $p$ -H<sub>2</sub>. Our main goal has

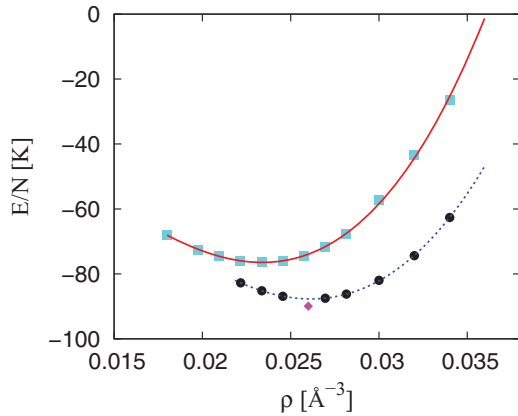


FIG. 1. (Color online) DMC energies per particle as a function of the density. Squares and circles correspond to the liquid and solid phases, respectively. Solid and dashed lines are the polynomial fits to the DMC energies for the liquid and solid, respectively. The diamond is the experimental energy of hcp molecular hydrogen from Ref. 43

been to know the properties of a hypothetical bulk liquid phase and compare them with the ones of the stable solid. In order to achieve reliable estimations of liquid  $p$ -H<sub>2</sub> it is crucial to work with a guiding wave function of liquid type, as we have discussed in the preceding section. Within the typical imaginary-time length of our simulations we have not seen the formation of any crystal structure [i.e., no signatures of Bragg peaks in the structure function  $S(k)$  have been registered so far].

In Fig. 1, we plot the DMC energies per particle of metastable liquid  $p$ -H<sub>2</sub> as a function of the density. For comparison, we also report the results obtained for the hcp crystal phase. Our hcp energies are in close agreement with the ones reported in Ref. 42 using the same Silvera-Goldman potential. In the figure, we also show the experimental estimation at  $T = 0$  K from Ref. 43,  $E/N = -89.9$  K, that lies a bit below our results. This is again in agreement with previous DMC results<sup>42</sup> which show that the experimental energy is, in absolute value, underestimated and overestimated by the Silvera-Goldman and Buck potential,<sup>44</sup> respectively. Our results for both phases are well reproduced by the polynomial law,

$$\frac{E}{N} = \left(\frac{E}{N}\right)_0 + A \left(\frac{\rho - \rho_0}{\rho_0}\right)^2 + B \left(\frac{\rho - \rho_0}{\rho_0}\right)^3, \quad (7)$$

$(E/N)_0$  and  $\rho_0$  being the equilibrium energy per particle and equilibrium density, respectively. These equations of state are shown in Fig. 1 with lines. The optimal parameters of the fits are as follows:  $\rho_0 = 0.026137(20) \text{ \AA}^{-3}$ ,  $(E/N)_0 = -87.702(37) \text{ K}$ ,  $A = 235(2) \text{ K}$ ,  $B = 140(10) \text{ K}$  for the solid, and  $\rho_0 = 0.023386(40) \text{ \AA}^{-3}$ ,  $(E/N)_0 = -76.465(51) \text{ K}$ ,  $A = 188(1) \text{ K}$ ,  $B = 131(10) \text{ K}$  for the liquid. As expected, our DMC results show that the solid phase is the stable one with a difference in energy per particle at the respective equilibrium points of  $\sim 10$  K, the equilibrium density of the liquid being  $\sim 10\%$  smaller than the solid one. The same trend was observed in a DMC simulation of two-dimensional  $p$ -H<sub>2</sub>, but there the differences were significantly smaller.<sup>45</sup> It is worth noticing that about one-half of the energy difference in the bulk systems comes from the decrease of the kinetic energy per particle

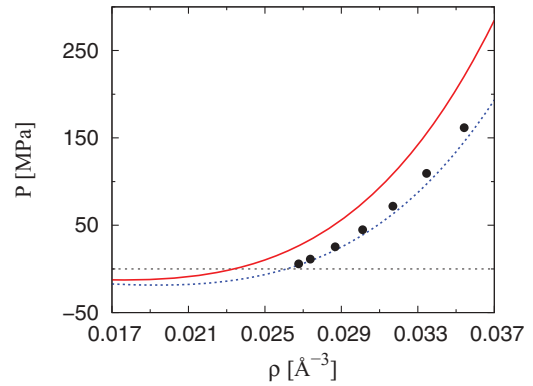


FIG. 2. (Color online) Pressure of the liquid (solid line) and solid (dashed line)  $p$ -H<sub>2</sub> phases as a function of the density. Experimental points for the solid phase<sup>46</sup> are shown as solid circles.

going from the liquid to the solid: At density  $\rho = 0.03 \text{ \AA}^{-3}$ , it amounts to 93.3(1) and to 89.5(1) K for the liquid and solid, respectively.

From the equations of state (7), it is easy to deduce the pressure of the system at any density using the relation  $P(\rho) = \rho^2[d(E/N)/d\rho]$ . The results obtained for metastable liquid and stable solid phases are shown in Fig. 2. As one can see, at a given density the pressure of the liquid is larger than the one of the solid mainly because of the different location of the equilibrium densities ( $P = 0$ ). The results for the solid are compared with experimental data from Ref. 46 showing good agreement especially for not very large pressures. The density at which the function  $P(\rho)$  has a zero slope defines the spinodal point; beyond this limit the system is no more thermodynamically stable as a homogeneous phase. At this point, the speed of sound  $c(\rho) = [m^{-1}(dP/d\rho)]^{1/2}$  becomes zero. Results for  $c(\rho)$  are shown for both phases in Fig. 3. The speed of sound decreases when the density is reduced and drops to zero at the spinodal point: [ $\rho_c = 0.0176(1) \text{ \AA}^{-3}$ ,  $P_c = -12.6(5) \text{ MPa}$ ] and [ $\rho_c = 0.0193(1) \text{ \AA}^{-3}$ ,  $P_c = -18.5(5) \text{ MPa}$ ] for liquid and solid, respectively.

DMC produces also accurate results for the structure of the bulk system. In Fig. 4, we show results for the two-body radial distribution function  $g(r)$  of the liquid  $p$ -H<sub>2</sub> phase for a set of densities. This function is proportional to the probability of finding two molecules separated by a distance  $r$ . Increasing the

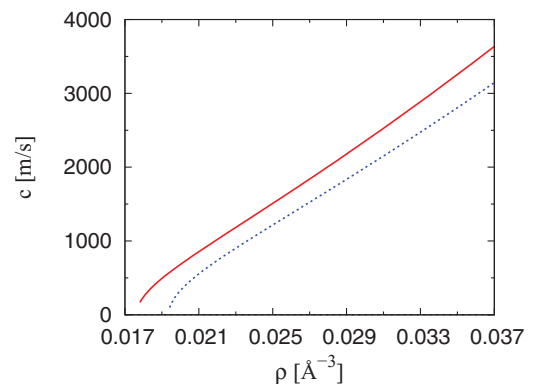


FIG. 3. (Color online) Speed of sound of the liquid (solid line) and solid (dashed line)  $p$ -H<sub>2</sub> phases as a function of the density.

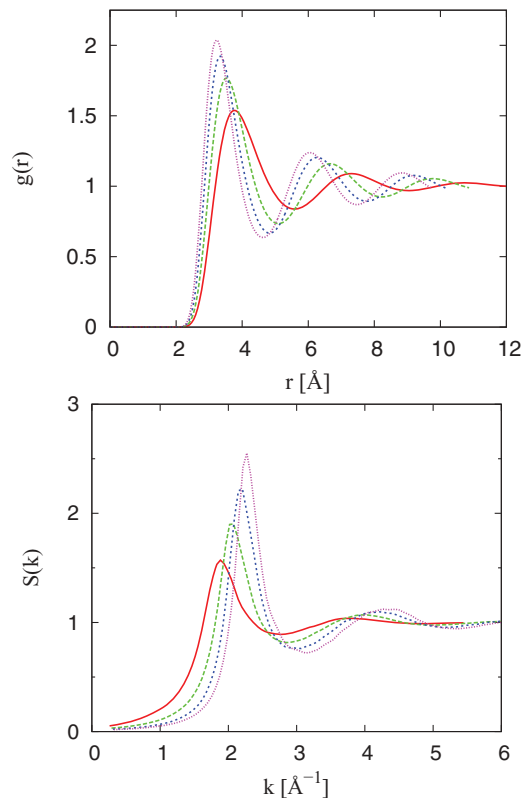


FIG. 4. (Color online) (Top) Two-body radial distribution function of the liquid  $p$ -H<sub>2</sub> phase at different densities: solid, long-dashed, short-dashed, and dotted lines stand for densities  $\rho = 0.0180, 0.0245, 0.0300,$  and  $0.0340 \text{ Å}^{-3}$ , respectively. (Bottom) Static structure factor of the liquid phase. Same densities and notation as in the top panel.

density, the main peak becomes higher and moves to shorter interparticle distances; at least three peaks are observed. All these features point to the picture of a very dense liquid, with much more structure than in stable liquid  $^4\text{He}$ . In the same Fig. 4, we show results for the static structure factor  $S(k)$ , related to  $g(r)$  by a Fourier transform. As one can see, the main peak increases quite fast with the density suggesting a highly structured metastable liquid. Nevertheless, we have not observed within the scale of the simulations the emergence of

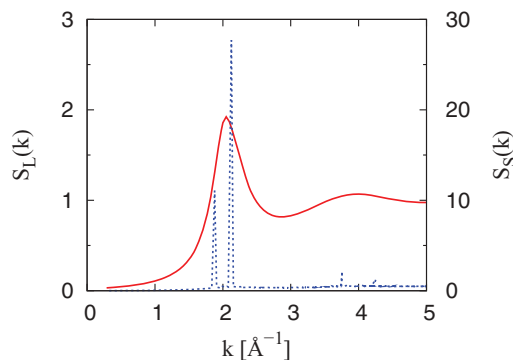


FIG. 5. (Color online) Static structure function of liquid and solid  $p$ -H<sub>2</sub> at density  $\rho = 0.0245 \text{ Å}^{-3}$ . The result for the liquid  $S_L(k)$  (left scale) is shown with a solid line; the one for the hcp solid  $S_S(k)$  (right scale) is shown with a dashed line.

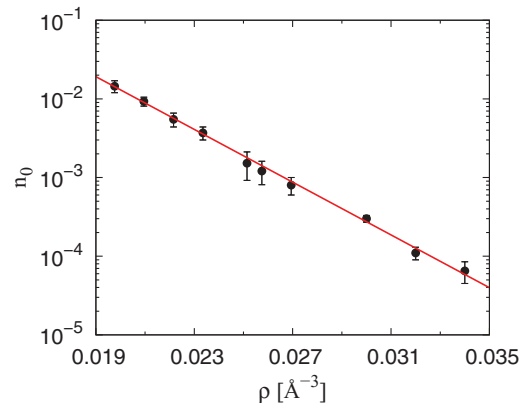


FIG. 6. (Color online) Condensate fraction of metastable liquid  $p$ -H<sub>2</sub> as a function of the density. The points are the DMC results and the line is an exponential fit to them.

any Bragg peak which would point to formation of crystallites in the simulation box. In Fig. 5, we illustrate the comparison between  $S(k)$  for the liquid and solid systems at a density  $\rho = 0.0245 \text{ Å}^{-3}$ , close to the equilibrium density of the liquid. The difference is the one expected between a liquid and a solid: oscillating function towards one at large  $k$  for the liquid and a sequence of Bragg peaks, corresponding to the hcp lattice, for the solid.

One of the most relevant properties of a superfluid is the mean occupation of the zero-momentum state (i.e., the condensate fraction  $n_0$ ). As is well known,  $n_0$  can be obtained from the asymptotic behavior of the one-body density matrix  $\rho_1(r)$ ,

$$n_0 = \lim_{r \rightarrow \infty} \rho_1(r), \quad (8)$$

with  $\rho_1(r)$  being obtained as the expectation value of the operator,

$$\left\langle \frac{\Phi(\mathbf{r}_1, \dots, \mathbf{r}_i + \mathbf{r}, \dots, \mathbf{r}_N)}{\Phi(\mathbf{r}_1, \dots, \mathbf{r}_N)} \right\rangle. \quad (9)$$

DMC results for the condensate fraction of liquid  $p$ -H<sub>2</sub> as a function of the density, obtained using the extrapolated estimator (there are no reliable pure estimators for nondiagonal operators), are shown in Fig. 6. The decrease of  $n_0$  with the density is well described by an exponential decay (line in the figure). The strong interactions induced by the deep attractive potential well produce a big depletion of the condensate state. At the equilibrium density, our estimation for the condensate fraction is  $n_0 = 0.0037(7)$ . This value is more than one order of magnitude smaller than the measured condensate fraction<sup>2</sup> of liquid  $^4\text{He}$  at equilibrium (0.08).

#### IV. SUPERFLUID TRANSITION TEMPERATURE

One of the main goals of our work has been to determine the temperature at which a disordered phase of  $p$ -H<sub>2</sub> becomes eventually superfluid. Recently, a similar approach has been used to study the superfluid properties of a glass phase of  $^4\text{He}$ ,<sup>33</sup> a system that has been named superglass and that it has been argued to be related with some of the effects observed in torsional oscillator experiments on solid  $^4\text{He}$ .

The first difficulty we have to deal with when investigating computationally a disordered phase of  $p$ -H<sub>2</sub> at low temperature is to provide a good equilibration of the system. The PIMC method, indeed, is aimed at studying the thermodynamic properties of quantum systems at thermal equilibrium. On the contrary, our purpose here is to study a configuration different from the one of minimum free energy, which for  $p$ -H<sub>2</sub> at low temperature is the crystalline one. In order to do that, it is fundamental to choose thoroughly the dimensions of the simulation box and the number of particles, which must not be commensurate with any crystalline lattice. In addition, it is important to choose a good initial configuration which evolves, as the Monte Carlo simulation goes on, towards a noncrystalline phase which remains metastable for a number of Monte Carlo steps large enough to get good statistics of the relevant quantities of the system. In this equilibration process, special attention must be paid to the thermalization of the polymers used within the PIMC formalism. A bad choice of initial conditions may cause the evolution of the system towards a configuration where the polymers representing each molecule are not allowed to spread and thus are not able to describe properly the zero-point motion of the molecules. This eventuality may represent a serious problem in our simulation, since we are mainly interested in the investigation of the superfluid properties of  $p$ -H<sub>2</sub>.

To check whether an equilibration scheme is efficient or not, it is important to monitor how the numerical estimations of the physical quantities change with the number of Monte Carlo steps. If we see that, as the simulation goes on, the computed variables do not show any evident trend but fluctuate around a certain value, we can conclude that the system has reached the metastability. To check if this eventual metastable phase is crystalline or not, we can calculate the static structure factor  $S(k)$  and observe if it presents the Bragg peaks typical of a crystal configuration.

We have used different technical schemes to get the desired metastable glass/liquid configuration. In many cases, we were not able to stabilize this phase and after some time the liquid froze. Finally, we managed to devise a successful approach that is based on the following two steps. In the first part, we perform the simulation of a fictitious system of quantum particles with a mass equal to the one of the  $p$ -H<sub>2</sub> molecules, but interacting through the <sup>4</sup>He-<sup>4</sup>He Aziz potential.<sup>47</sup> Compared with the H<sub>2</sub> Silvera-Goldman pair interaction, the Aziz potential does not present a so deep attractive well and thus it is not able to freeze the system. Once this fictitious system is equilibrated, we change the Aziz interaction by the Silvera-Goldman one and equilibrate again towards the metastable  $p$ -H<sub>2</sub> phase. At all the temperatures we consider in our study, we have verified that the superfluid properties of  $p$ -H<sub>2</sub> do not depend on the fact that permutations are allowed or not in the first step of the equilibration. To test this equilibration scheme, we have performed a simulation of  $N = 100$   $p$ -H<sub>2</sub> molecules interacting through the Silvera-Goldman potential,<sup>34</sup> inside a cubic box at the equilibrium density of the liquid phase at zero temperature (see Sec. III),  $\rho = 0.0234 \text{ \AA}^{-3}$ . For a preliminary test, we choose to perform the PIMC simulation at temperature  $T = 10$  K, that is an intermediate temperature below the freezing temperature, where the liquid phase should

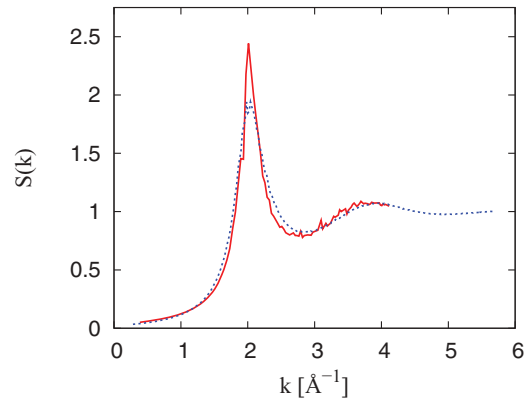


FIG. 7. (Color online) Static structure factor  $S(k)$  of metastable bulk  $p$ -H<sub>2</sub> at  $T = 10$  K obtained with PIMC (solid line). This result is compared with the static structure factor of liquid  $p$ -H<sub>2</sub> at zero temperature obtained with DMC (dotted line).

be unstable, but above the estimated superfluid transition temperature, in order to make the simulation easier. It is worth noticing that after equilibration the glass phase is better sampled, and thus crystallization is avoided, when the center of mass of all the polymers are moved simultaneously and accepted or not collectively by a single Metropolis step.

In Fig. 7, we have plotted the static structure factor  $S(k)$  of the metastable phase and compared it with the same quantity computed for the liquid phase with DMC. We can see that the curve obtained at  $T = 10$  K presents the first peak at the same  $k$  as the  $S(k)$  of the liquid and follows the same behavior up to the second maximum which is at  $k \simeq 4 \text{ \AA}^{-1}$ . Even though the PIMC calculation gives a peak which is higher and narrower than the peak obtained with DMC, and indicates that the PIMC configurations are slightly more structured than the DMC ones, we can conclude that our equilibration scheme is able to create a metastable liquid phase, at least in the range of intermediate temperature below the freezing point  $T_f$  and above the expected superfluid transition  $T_\lambda$ .

Since our main purpose is to localize the superfluid transition of this noncrystalline phase, it is worth testing this equilibration scheme at lower temperatures, closer to the expected  $T_\lambda$ . For this reason, we have performed a simulation with  $N = 90$   $p$ -H<sub>2</sub> molecules at the same density,  $\rho = 0.0234 \text{ \AA}^{-3}$ , but at a lower temperature,  $T = 2$  K. Once the mean value of the energy was stable, we computed the static structure factor  $S(k)$ . The result is shown in Fig. 8, in comparison with the static structure factor of the zero-temperature liquid. As we can see,  $S(k)$  obtained in the PIMC simulation presents narrow maxima in the range of small  $k$  and is different from the typical  $S(k)$  of a liquid phase. However, these maxima tend to disappear at higher  $k$  and their height is much lower than the height of the Bragg peaks appearing in the  $S(k)$  of a crystal. This indicates that the system simulated with PIMC has relaxed to a glass phase, which is structured at short range but lacks the long-range coordination typical of the crystal structures.

Even if a glassy configuration can make the diffusion of particles harder, the lack of long-range coordination makes possible the appearance of off-diagonal long-range order and

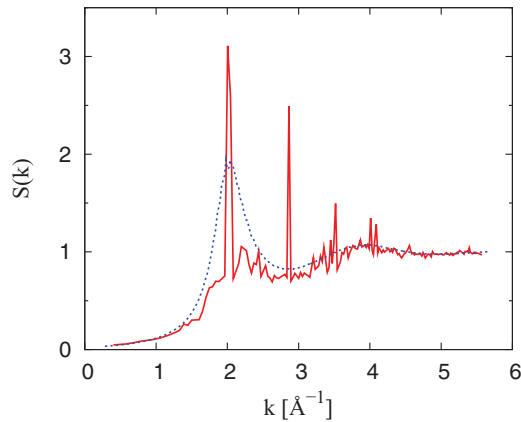


FIG. 8. (Color online) Static structure factor  $S(k)$  of metastable bulk  $p$ -H<sub>2</sub> at  $T = 2$  K obtained with PIMC (solid line). For comparison, we also show the  $S(k)$  of liquid  $p$ -H<sub>2</sub> at zero temperature obtained with DMC (dotted line).

it is worth studying the superfluid properties of this phase. To do that, we have studied the temperature dependence of the one-body density matrix  $\rho_1(r)$ . The first simulation has been performed at  $T = 2$  K, using  $N = 90$   $p$ -H<sub>2</sub> molecules inside a cubic box at density  $\rho = 0.0234 \text{ \AA}^{-3}$ . The result for  $\rho_1(r)$  obtained in this simulation is shown in Fig. 9: At  $T = 2$  K, we can clearly see an exponential decay of  $\rho_1(r)$  at large  $r$ , indicating that Bose-Einstein condensation is not present in the system. In fact, we have noticed that in this calculation the swap update (the update responsible for bosonic exchanges in our PIMC sampling) has a very low acceptance rate and does not allow the formation of long-permutation cycles with a nonzero winding number. Nevertheless, one can think that the low acceptance of the swap update is a consequence of the difficulties in the sampling of the coordinates due to the strength of the intermolecular potential. We may therefore suspect that the system remains stuck in a configuration without permutation because of sampling issues. To be sure about our result, we have performed another simulation of the same system but starting from an initial configuration

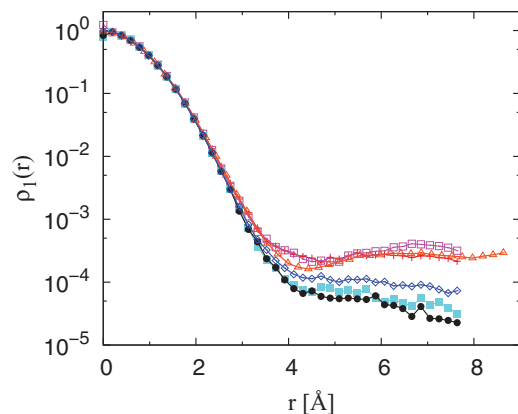


FIG. 9. (Color online) One-body density matrix  $\rho_1(r)$  for glass  $p$ -H<sub>2</sub> at density  $\rho = 0.0234 \text{ \AA}^{-3}$  and at different temperatures.  $T = 0.7$  K (crosses),  $T = 1.0$  K (open squares),  $T = 1.0$  K, and  $N = 130$  (triangles),  $T = 1.2$  K (diamonds),  $T = 1.5$  K (solid squares), and  $T = 2.0$  K (circles).

presenting a nonzero winding number. To create this initial configuration, we have allowed particles to permute even in the fictitious simulation used to equilibrate the system. When we start the PIMC simulation of  $p$ -H<sub>2</sub> from the permuted configuration, we see that the percentage of particles involved in bosonic exchanges tends to decrease and, at the end of the equilibration, the system has relaxed to a phase presenting zero winding number (i.e., the superfluid density is zero). This last result confirms our conclusion that the  $p$ -H<sub>2</sub> glass we simulate is not superfluid at  $T = 2$  K.

In Fig. 9, we have also shown  $\rho_1(r)$  estimated at other temperatures. At each of the temperatures studied, we have performed simulations starting both from a permuted and a nonpermuted configuration, observing that once the system has been equilibrated the results for  $\rho_1(r)$  do not depend on the initial configuration. From the comparison of the curves at different temperatures, we can easily see a change of the behavior of  $\rho_1$  at large  $r$  as the temperature decreases: this indicates that, at temperatures close to  $T = 1$  K, the system presents a transition to a superfluid phase presenting off-diagonal long-range order. The condensate fraction at low temperature is  $n_0 \sim 3 \times 10^{-4}$ , appreciably smaller than the DMC estimation for the liquid phase at  $T = 0$ . The observation of a finite value for the condensate fraction at  $T = 1$  K agrees with the measure of a finite value for the superfluid density. Our results show that the superfluid density, derived from the winding number estimation, is zero within our numerical uncertainty for  $T > 1.2$  K and at  $T = 1$  K is already  $\rho_s/\rho = 0.36 \pm 0.08$ . In order to give a more precise estimation of the superfluid transition temperature  $T_\lambda$ , it would be necessary to perform a pertinent finite-size scaling study. However, the achievement of the metastable state is quite hard for systems made up of more than  $\sim 100$  molecules. In our study, we have been able to stabilize the amorphous phase for a system made up of 130  $p$ -H<sub>2</sub> molecules at  $T = 1$  K. The result for  $\rho_1(r)$  is also shown in Fig. 9. We notice that this result is in agreement with the one calculated for the smaller system of 90  $p$ -H<sub>2</sub> molecules at the same temperature, supporting our conclusion that the system has undergone a superfluid transition. At higher temperatures, instead, the system made up of 130  $p$ -H<sub>2</sub> molecules relaxes to a crystalline phase and it has not been possible to calculate  $\rho_1(r)$  for the amorphous configuration. This result seems to indicate that the disordered phase is somehow “more stable” at lower temperature, when the  $p$ -H<sub>2</sub> molecules begin to permute. A similar behavior has also been found in PIMC simulations of small  $p$ -H<sub>2</sub> clusters.<sup>21</sup>

## V. CONCLUSIONS

We have carried out extensive quantum Monte Carlo calculations of  $p$ -H<sub>2</sub> at temperatures well below its solidification point. Our interest has been to know better the properties of the metastable liquid/glass phase at very low temperatures and to determine where the superfluid transition is expected to appear. In the limit of zero temperature we have used the DMC method, which is a very efficient tool to sample this metastable phase through the use of a proper guiding wave function. The results point to a very structured liquid with a large depletion of the condensate fraction, significantly larger than in stable liquid <sup>4</sup>He.

Our estimation of  $T_\lambda \sim 1$  K is slightly smaller than the prediction obtained using a phenomenological approach<sup>8</sup> for which, at the density  $\rho = 0.0234 \text{ \AA}^{-3}$  studied in our simulations, the transition temperature is estimated to be  $T_\lambda \sim 1.7$  K. It is also interesting to notice that our result for  $T_\lambda$  is quite close to the temperatures at which, according to PIMC simulations, superfluid effects should appear in small  $p$ -H<sub>2</sub> clusters.<sup>20,21</sup> These calculations show that clusters made of  $N \leq 20$   $p$ -H<sub>2</sub> molecules exhibit a nonzero superfluid fraction below  $T \sim 2$  K. This transition temperature depends on the dimension of the cluster, decreasing when the number of molecules increases. However, it is difficult to hypothesize on the superfluid behavior of large enough  $p$ -H<sub>2</sub> systems from the simulation of small clusters, because the calculated superfluid fraction  $\rho_s$  is significantly depressed when the number of

molecules becomes  $N \geq 30$ . This unexpected behavior of  $\rho_s$  with  $N$  has been explained by relating the changes in the superfluid properties to structural changes that make the molecules arrange according to a solidlike configuration when the dimension of the cluster becomes large. In our simulation of bulk glass  $p$ -H<sub>2</sub>, we have been able to frustrate crystallization with an efficient equilibration of the system and to measure finite values of both the condensate fraction and superfluid density.

#### ACKNOWLEDGMENTS

The authors acknowledge partial financial support from the DGI (Spain) Grant No. FIS2011-25275 and Generalitat de Catalunya Grant No. 2009SGR-1003.

- 
- <sup>1</sup>L. Pitaevskii and S. Stringari, *Bose-Einstein Condensation* (Clarendon Press, Oxford, 2003).
- <sup>2</sup>H. R. Glyde, S. O. Diallo, R. T. Azuah, O. Kirichek, and J. W. Taylor, *Phys. Rev. B* **83**, 100507 (2011).
- <sup>3</sup>R. M. Panoff and J. W. Clark, *Phys. Rev. B* **36**, 5527 (1987).
- <sup>4</sup>I. Bešlić, L. V. Markić, and J. Boronat, *Phys. Rev. B* **80**, 134506 (2009).
- <sup>5</sup>D. G. Fried, T. C. Killian, L. Willmann, D. Landhuis, S. C. Moss, D. Kleppner, and T. J. Greytak, *Phys. Rev. Lett.* **81**, 3811 (1998).
- <sup>6</sup>I. F. Silvera, *Rev. Mod. Phys.* **52**, 393 (1980).
- <sup>7</sup>V. L. Ginzburg and A. A. Sobyanin, *JEPT Lett.* **15**, 242 (1972).
- <sup>8</sup>S. M. Apenko, *Phys. Rev. B* **60**, 3052 (1999).
- <sup>9</sup>H. J. Maris, G. M. Seidel, and T. E. Huber, *J. Low Temp. Phys.* **51**, 471 (1983).
- <sup>10</sup>M. Kühnel, J. M. Fernández, G. Tejada, A. Kalinin, S. Montero, and R. E. Grisenti, *Phys. Rev. Lett.* **106**, 245301 (2011).
- <sup>11</sup>H. J. Maris, G. M. Seidel, and F. I. B. Williams, *Phys. Rev. B* **36**, 6799 (1987).
- <sup>12</sup>V. S. Vorob'ev and S. P. Malysenko, *J. Phys.: Condens. Matter* **12**, 5071 (2000).
- <sup>13</sup>R. E. Grisenti, R. A. Costa Fraga, N. Petridis, R. Dörner, and J. Deppe, *Europhys. Lett.* **73**, 540 (2006).
- <sup>14</sup>S. Grebenev, B. Sartakov, J. P. Toennies, and A. F. Vilesov, *Science* **289**, 1532 (2000).
- <sup>15</sup>H. Li, R. J. Le Roy, P. N. Roy, and A. R. W. McKellar, *Phys. Rev. Lett.* **105**, 133401 (2010).
- <sup>16</sup>K. Kuyanov-Prozument and A. F. Vilesov, *Phys. Rev. Lett.* **101**, 205301 (2008).
- <sup>17</sup>M. C. Gordillo and D. M. Ceperley, *Phys. Rev. Lett.* **79**, 3010 (1997).
- <sup>18</sup>M. Boninsegni, *New J. Phys.* **7**, 78 (2005).
- <sup>19</sup>M. C. Gordillo, J. Boronat, and J. Casulleras, *Phys. Rev. Lett.* **85**, 2348 (2000).
- <sup>20</sup>P. Sindzingre, D. M. Ceperley, and M. L. Klein, *Phys. Rev. Lett.* **67**, 1871 (1991).
- <sup>21</sup>F. Mezzacapo and M. Boninsegni, *Phys. Rev. Lett.* **97**, 045301 (2006).
- <sup>22</sup>F. Mezzacapo and M. Boninsegni, *Phys. Rev. A* **75**, 033201 (2007).
- <sup>23</sup>S. A. Khairallah, M. B. Sevryuk, D. M. Ceperley, and J. P. Toennies, *Phys. Rev. Lett.* **98**, 183401 (2007).
- <sup>24</sup>F. Mezzacapo and M. Boninsegni, *Phys. Rev. Lett.* **100**, 145301 (2008).
- <sup>25</sup>E. Sola and J. Boronat, *J. Phys. Chem. A* **115**, 7071 (2011).
- <sup>26</sup>R. Guardiola and J. Navarro, *Cent. Eur. J. Phys.* **6**, 33 (2008).
- <sup>27</sup>J. E. Cuervo and P. N. Roy, *J. Chem. Phys.* **125**, 124314 (2006).
- <sup>28</sup>J. E. Cuervo and P. N. Roy, *J. Chem. Phys.* **128**, 224509 (2008).
- <sup>29</sup>J. E. Cuervo and P. N. Roy, *J. Chem. Phys.* **131**, 114302 (2009).
- <sup>30</sup>Y. Kwon and K. B. Whaley, *Phys. Rev. Lett.* **89**, 273401 (2002).
- <sup>31</sup>F. Paesani, R. E. Zillich, Y. Kwon, and K. B. Whaley, *J. Chem. Phys.* **122**, 181106 (2005).
- <sup>32</sup>Y. Kwon and K. B. Whaley, *J. Low Temp. Phys.* **140**, 227 (2005).
- <sup>33</sup>M. Boninsegni, N. Prokof'ev, and B. Svistunov, *Phys. Rev. Lett.* **96**, 105301 (2006).
- <sup>34</sup>I. F. Silvera and V. V. Goldman, *J. Chem. Phys.* **69**, 4209 (1978).
- <sup>35</sup>J. Boronat and J. Casulleras, *Phys. Rev. B* **49**, 8920 (1994).
- <sup>36</sup>J. Casulleras and J. Boronat, *Phys. Rev. B* **52**, 3654 (1995).
- <sup>37</sup>L. Reatto, *Nucl. Phys. A* **328**, 253 (1979).
- <sup>38</sup>D. M. Ceperley, *Rev. Mod. Phys.* **67**, 279 (1995).
- <sup>39</sup>S. A. Chin and C. R. Chen, *J. Chem. Phys.* **117**, 1409 (2002).
- <sup>40</sup>K. Sakkos, J. Casulleras, and J. Boronat, *J. Chem. Phys.* **130**, 204109 (2009).
- <sup>41</sup>M. Boninsegni, N. V. Prokof'ev, and B. V. Svistunov, *Phys. Rev. E* **74**, 036701 (2006).
- <sup>42</sup>F. Operetto and F. Pederiva, *Phys. Rev. B* **73**, 184124 (2006).
- <sup>43</sup>O. Schnepp, *Phys. Rev. A* **2**, 2574 (1970).
- <sup>44</sup>U. Buck, F. Huisken, A. Kohlhase, D. Otten, and J. Schaefer, *J. Chem. Phys.* **78**, 4439 (1983); M. J. Norman, R. O. Watts, and U. Buck, *ibid.* **81**, 3500 (1984).
- <sup>45</sup>C. Cazorla and J. Boronat, *Phys. Rev. B* **78**, 134509 (2008).
- <sup>46</sup>A. Driessen, J. A. de Waal, and I. F. Silvera, *J. Low Temp. Phys.* **34**, 255 (1979).
- <sup>47</sup>R. A. Aziz, F. R. W. McCourt, and C. C. K. Wong, *Mol. Phys.* **61**, 1487 (1987).